Water Research 189 (2021) 116559

Contents lists available at ScienceDirect

Water Research

journal homepage: www.elsevier.com/locate/watres

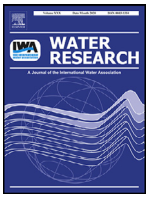

Paper-based nanosensors to evaluate community-wide illicit drug use for wastewater-based epidemiology

Kang Mao[a,d], Zhugen Yang[b,*], Hua Zhang[a,*], Xiqing Li[c,*], Jonathan M. Cooper[d]

[a] State Key Laboratory of Environmental Geochemistry, Institute of Geochemistry, Chinese Academy of Sciences, Guiyang, 550081, China
[b] Cranfield Water Science Institute, Cranfield University, Cranfield, MK43 0AL, United Kingdom
[c] Laboratory for Earth Surface Processes, College of Urban and Environmental Sciences, Peking University, Beijing 100871, China
[d] Division of Biomedical Engineering, James Watt School of Engineering, University of Glasgow, G12 8LT, Glasgow, United Kingdom

ARTICLE INFO

Article history:
Received 2 August 2020
Revised 20 October 2020
Accepted 22 October 2020
Available online 23 October 2020

Keywords:
Wastewater-based epidemiology
SERS
Nanosensors
Illicit drugs
Public health

ABSTRACT

Wastewater-based epidemiology (WBE) is a powerful technique for monitoring illicit drugs of abuse in the community. Here, we report upon a surface-enhanced Raman spectroscopy (SERS) sensor for the sensitive and selective detection of methamphetamine based upon the assembly of noble metal core-shell nanoparticles on a bespoke glassy nanofibrous electrospun paper matrix. The hierarchical structure of the fibrous paper, modified with the synthesized Au@Ag core-shells (Au@Ag) gave strong SERS signalling, enabling us to evaluate the community-wide prevalence of methamphetamine in wastewater treatment plants within Beijing. We show that, when normalized for the daily flow of the wastewater treatment plants and for population density, higher mass loads of drugs are generally found in sewage influent from urban areas, implying greater local methamphetamine usage than that in less populated areas. The user-friendly and disposable paper sensors demonstrate the applicability of rapid on-site illicit drug detection, illustrating the application to wastewater-based epidemiology, which has the potential to inform government agencies regarding societal interventions.

1. Introduction

Worldwide illicit drug use has increased significantly, generating global concern around both public health as well as national and international security (Niaz et al., 2017). In particular, methamphetamine, as one of the most widely used illicit drugs, is currently the most widely abused drug in China (Du et al., 2015; Niaz et al., 2017). The use of methamphetamine has important societal consequences, including the loss of livelihoods, higher incidences of local and organized crime, and increased healthcare costs with associated morbidities and mortalities (Niaz et al., 2017). To date, traditional methods for monitoring community drug use have been based largely upon population surveys, which are time-consuming and may be inaccurate (Zuccato et al., 2008). In the past decade, a new approach, namely, wastewater-based epidemiology (WBE), has emerged as a powerful, near-real-time and cost-effective tool both for the evaluation of illicit drug consumption (Castrignanò et al., 2018; Du et al., 2019) or toxic substance exposure (Markosian and Mirzoyan, 2019; Rousis et al., 2017) as well as, most recently, for the early warning of infectious disease outbreaks (Peccia et al., 2020; Sims and Kasprzyk-Hordern, 2020).

Recently, such measurements of a community's drug consumption have been demonstrated through the quantification of the chemical residues and/or metabolites that enter the urban sewers from urine or faeces, although these methods have always used traditional centralized laboratory testing based upon chromatographic separation methods coupled with mass spectrometry (Bell and Sirimuthu, 2008; Castiglioni et al., 2013, 2015; Chen et al., 2013; Cyranoski, 2018; Du et al., 2015, 2017; Harman et al., 2011; Reid et al., 2014; Zuccato et al., 2005). The analytic approach needs to consider the population serviced, the stability of drug residues, the rates of drug excretion and wastewater volumes (Chen et al., 2013; Harman et al., 2011; Zuccato et al., 2005). By analysing wastewater collected at treatment plants (Chen et al., 2013; Harman et al., 2011; Reid et al., 2014), the community-wide use of drugs including antibiotics (Reid et al., 2014) and alcohol (Cyranoski, 2018) can has been evaluated. This method has also been demonstrated as an innovative and promising tool for the evaluation of recent trends in illicit drug use in many countries (Castiglioni et al., 2013, 2015; Du et al., 2015, 2017).

---

* Corresponding authors.
E-mail addresses: zhugen.yang@cranfield.ac.uk (Z. Yang), zhanghua@mail.gyig.ac.cn (H. Zhang), xli@urban.pku.edu.cn (X. Li).

https://doi.org/10.1016/j.watres.2020.116559

The use of chromatographic separation methods coupled with mass spectrometry (e.g., triple quadrupole instruments) provides a robust, sensitive and selective analytic approach (Bell and Sirimuthu, 2008), in which chemical compounds or their metabolites present in wastewater serve as biomarkers, quantified using an internal reference such as a deuterated analogue (Bell and Sirimuthu, 2008). Non-targeted analysis is usually undertaken by high-resolution mass spectrometry (Harman et al., 2011), a the method which involves complex sample preparation from sewage, as well as the high cost of analysis with a requirement for trained technicians. As a consequence, there is now a need for novel analytical tools to perform rapid and on-site analysis of wastewater with minimal sample processing by less skilled personnel.

We have recently demonstrated aptamer sensors for the electrochemical detection of cocaine (Yang et al., 2016) and for the colorimetric detection of methamphetamine (Mao et al., 2019). Building upon this experience, we believe that rapid monitoring of sewage minimizes uncertainty arising from the low stability of certain targets (Du et al., 2015; Kneipp et al., 2008; Zuccato et al., 2005).

Surface-enhanced Raman spectroscopy (SERS) is a powerful spectroscopic technique for label-free detection of (bio)chemical species, enabling the analysis of a spectroscopic fingerprint of each molecule (Brown and Milton, 2008; Ji et al., 2012). This approach has already been confirmed to be an attractive method for the monitoring of chemical pollutants (Brown and Milton, 2008) and pesticides (Li et al., 2017) present in the environment at low concentrations. The key to this technique is the electromagnetic enhancement afforded by noble metal nanostructures (Lin et al., 2016; Xie et al., 2011). Although SERS analysis holds potential to achieve ultrasensitive detection (Huang et al., 2020; Ren et al., 2011), its broader applicability has been hindered by problems associated with both sample preparation and reproducibility of the signal generated at the SERS-active sensor substrate (Su et al., 2017); both being key requirements for practical implementation (Kudelski, 2005; Reilly et al., 2007). Thus, techniques including the creation of colloidal suspensions of metal nanocrystals using chemical synthesis (Wang et al., 2005; Yap et al., 2012), electrochemically nano-textured metal surfaces (Cheng et al., 2010), regularly patterned metal particles using vapour deposition (Reilly et al., 2007), lithographic techniques (Wang et al., 2005), and template-directed self-assembly (Yap et al., 2012) have all been developed to manufacture stable and sensitive sensing surfaces. The wide variety of different techniques currently available (Cheng et al., 2010) includes those for the fabrication of well-ordered periodic silver or gold nanoparticle arrays, which enable precise control over the shape, size, and organization of the metal nanostructures (He et al., 2009). Generally, SERS substrates obtained by these techniques show a large Raman enhancement and high reproducibility, enabling single molecule detection capable of identifying analytes at trace levels (Ahmed and Gordon, 2012).

Paper-based SERS substrates for on-site analysis of real samples (Abbas et al., 2013; Ahmed and Gordon, 2012; He et al., 2009; Polavarapu and Liz-Marzán, 2013; Polavarapu et al., 2014; Yu and White, 2010) provide a versatile and low-cost alternative and have attracted increasing interest in recent years for the development of portable miniaturized devices suitable for on-site analysis and testing (Martinez et al., 2008, 2010). Paper-based SERS substrates have the advantage that they can wick the samples by capillary forces, providing chromatographic sample preparation, filtration and fluid movement simultaneously (Polavarapu and Liz-Marzán, 2013). The paper matrix can also be adapted to provide visual/optical or electrochemical measurements (and can be easily disposed of at the end of the analysis) (Mao et al., 2020).

Recent studies have demonstrated the fabrication of inexpensive SERS substrates on paper, such as filter paper (Abbas et al., 2013), photocopy paper (Polavarapu et al., 2014), and cellulose paper (Yu and White, 2010), by printing (Yu and White, 2010), dip-coating gold nanorods (Lee et al., 2010), and *in situ* growth (Cheng et al., 2011) and filtration (Zhang et al., 2015). Despite these advances, there remain important limitations in the use of these paper-based sensors, including the high background Raman interference in the SERS detection observed in many commercially available papers. Furthermore, the inhomogeneous and discrete distribution of nanostructures on paper has meant that many techniques have only moderate sensitivities in the nM range (Zhang et al., 2015). In order to improve the signal readout, large sample volumes (e.g., litre level) have been needed to accumulate molecular targets in the detection zone, a task that is often impractical (Lee et al., 2011; Meng et al., 2013; Zhang et al., 2015).

The development of effective and simple production of closely-packed nanostructure arrays, uniformly distributed on the paper surface for signal analysis, also remains an important challenge. In order to overcome this obstacle, most recently, Xu et al. (2019) reported the SERS detection of methyl blue (MB), an organic pollutant in wastewater, using ZnO@Au nanorods as the substrate. Similarly, Lee et al. (2017) demonstrated the use of paper as a substrate for SERS detection of two toxic drugs (4-aminobenzoic acid and pyrocatechol) in “model” wastewater samples, with sensitivities as low as nM (equivalent to 150 ppt).

To our knowledge, rapid SERS detection using paper as a substrate to address WBE in the community for the evaluation of illicit drug use trends in real samples has not been reported. Here, we demonstrate a new, bespoke, paper-based SERS substrate created by the assembly of noble metal core-shell nanoparticles on modified electrospun glass nanofibrous paper (GNFP). The sensors were used for the detection of methamphetamine in water samples, including surface water and wastewater in different areas within Beijing (Fig. 1). The objectives of this study were to synthesize Au@Ag core-shells by seeded growth, which exhibit high SERS enhancement and construct a novel paper-based SERS substrate with the nanoparticles immobilized on a nanofibrous paper functionalized with poly-L-lysine (pLL). Finally we used this novel paper-based SERS substrate for methamphetamine detection in real surface and wastewater samples, which was compared to mass spectrometry as a gold-standard reference technique in order to evaluate community drug consumption with SERS sensors at wastewater treatment plants in Beijing. The sensor provides a potential tool for rapid on-site analysis of sewage to identify spatio-temporal variations in local trends in drug use.

2. Experimental section

2.1. Preparation of glass nanofibrous paper-based SERS substrates

Synthesis of Au@Ag core-shell nanoparticles: Gold nanoparticles (AuNPs) were prepared by reduction of gold(III) chloride hydrate with trisodium citrate using a procedure adapted from the literature (Shen et al., 2010). Briefly, 50 mL of 0.01% (w/w) $HAuCl_4$ was reduced by 750 μL of 1% (w/w) trisodium citrate solution at 100 °C under vigorous magnetic stirring for 20 min until the solution turned light red. The prepared AuNPs were used as seed particles. A total of 600 μL of $AgNO_3$ solution (0.5%, w/w) was added to 100 mL of the boiling gold seed solution. Afterwards, 1 mL of sodium citrate solution (1%, w/w) was added dropwise as the reducing agent with stirring. The solution was boiled for 1 h and then cooled to room temperature.

Fabrication of Au@Ag-pLL on paper: GNFP (8 mm × 8 mm) was first cleaned exhaustively through a series of sequential washing steps with ultrapure water, acetone, ethanol and ultrapure water (each for 10 min) prior to drying at 60 °C in the oven. The paper was then immersed in 0.1 wt% pLL solution for 10 min and

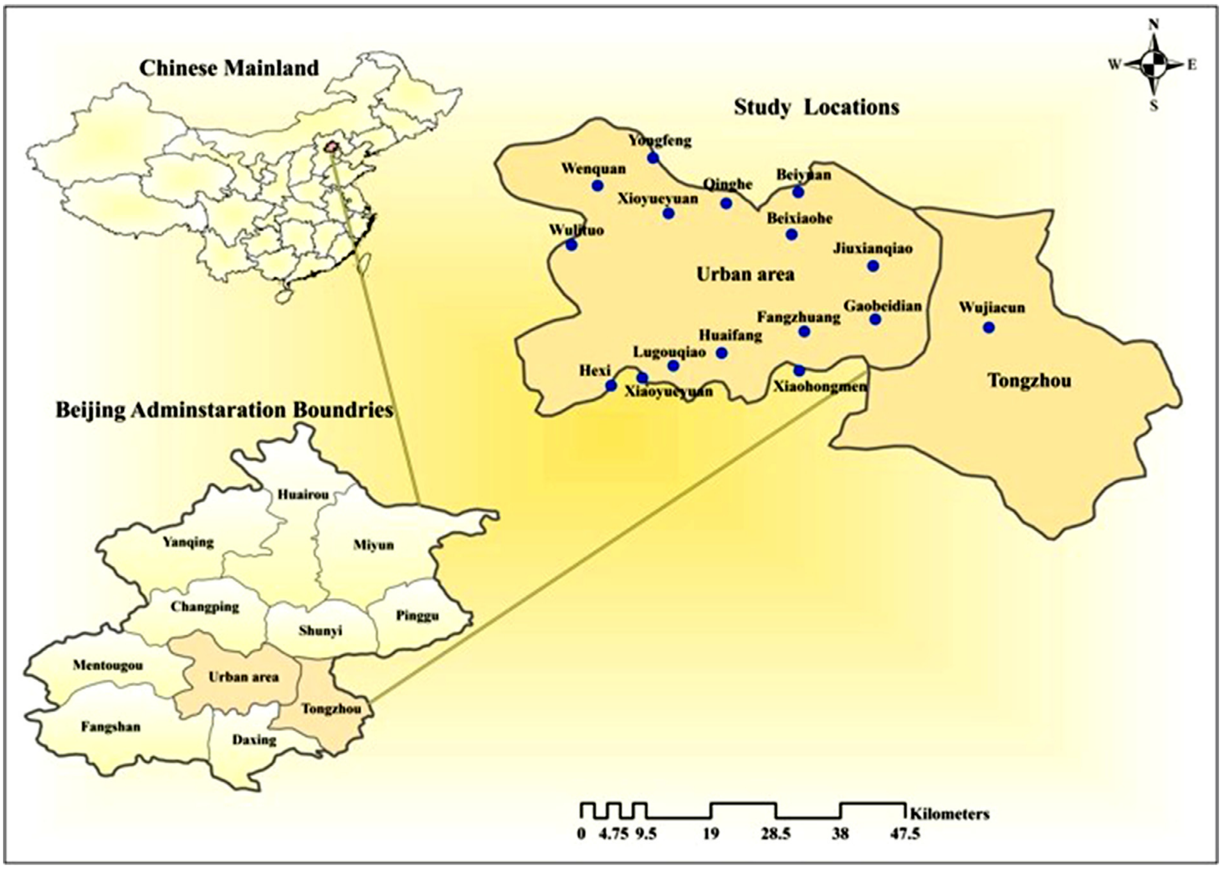

Fig. 1. Locations of the sixteen wastewater treatment plants in the urban area of Beijing**. The study locations were abbreviated as follows:** FZ, Fangzhuang; XHM, Xiaohongmen; HX, Hexi; WLT, Wulituo; LGQ, Lu**gouqiao; BY, Beiyuan; GBD, Gaobeidian; QH, Qinghe; WJC, Wujiacun; XJH, Xioajiahe; JXQ, Jiuxianqiao; BXH, Beixiaohe; WQ, Wenquan; XYY, Xiaoyueyuan; HF, Huaifang; YF, Yongfeng**).

rinsed in water, with any remaining fluid gently blown away under a stream of pure nitrogen gas. The pLL layer-coated GNFP was then immersed into a solution containing the synthesized Au@Ag core-shell colloid for 30 h. Au@Ag core-shell nanoparticles assembled on the surface of the nanofibrous paper due to local electrostatic interactions with pLL. Finally, the paper was washed with phosphate buffer (0.01 mM, pH 7.0) and dried in a stream of nitrogen gas. The substrates were characterized by both low-magnification and high-magnification field emission scanning electron microscopy (FE-SEM), as shown in Fig. 2.

2.2. Analytical performance of the novel SERS sensors

To demonstrate the quantitative capability of this SERS-active sensor, experimental samples were prepared as follows: crystal violet (CV) solids were dissolved in ethyl alcohol without any further purification to obtain a 1 mM stock solution. Then, CV standards were prepared using serial dilutions of the stock solution with ethyl alcohol. Similarly, standards of methamphetamine were prepared, again by serial dilution of a 100 ppm stock solution with deionized water, giving a series of methamphetamine standards at 0.01, 0.1, 1.0, 10.0, 100.0, 1000.0, and 10,000.0 ppb. These standards were used to determine key analytical performance metrics including the limit of detection and linear range.

2.3. Detection of illicit drugs in water samples

In order to evaluate the feasibility of detecting methamphetamine in real samples, concentrations in surface and wastewater samples were determined using SERS, and these samples were also measured using conventional instrumentation, namely, liquid chromatography-mass spectrometry (LC-MS). Surface water samples were collected from two rivers (the Pearl River in Guangdong Province and the Wanquan River in the City of Beijing) and from Weiming Lake in Beijing (see the supporting information for detailed sample collection information). In addition, wastewater was collected (as both influent and effluent) from sixteen domestic wastewater treatment plants (Fangzhuang, Xiaohongmen, Hexi, Wulituo, Lugouqiao, Beiyuan, Gaobeidian, Qinghe, Wujiacun, Xioajiahe, Jiuxianqiao, Beixiaohe, Wenquan, Xiaoyueyuan, Huaifang, and Yongfeng) located in the urban area of Beijing (Fig. 1). Sampling was conducted during summer. Each treatment plant was sampled for 4 consecutive days over a period of 24 h, and the samples were combined for measurement (detailed in the supporting information).

SERS analysis: Two hundred millilitres of wastewater was processed on-site by first acidifying the sample (by adding 10 drops of HCl, pH~2) and then filtering using a 0.22 μm membrane to remove solid debris. Purification and enrichment were performed using a standard 3 mL cationic solid-phase extraction cartridge from AFFINISEP (Paris, France), pre-equilibrated using 1 mL of acetonitrile (AcN) and 2 mL of water, as follows: sample loading (of the 200 mL of filtered wastewater); washing (for removal of interferences) in 3 mL of water and 3 mL of water/AcN (60/40, v/v); drying for 30 s prior to elution (in 2 mL of methanol (MeOH) containing 2% formic acid); and finally, analysis by SERS.

LC-MS analysis: First, 200 mL of each sample was filtered using 0.22 μm membrane filters to remove solid particles and then stored for reference laboratory analysis. An Oasis MCX cartridge from Waters (Milford, USA) was pre-conditioned in sequence with 6 mL of MeOH, 4 mL of deionized water, and 4 mL of deionized

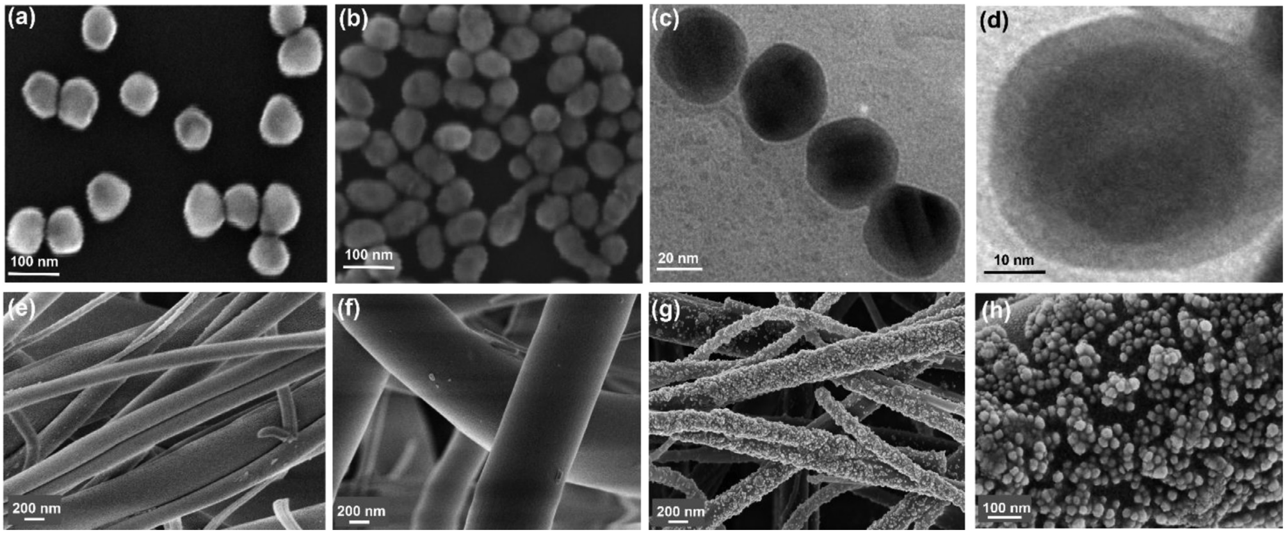

Fig. 2. Evaluation and characterization of Au@Ag assembled on the glass nanofibrous paper substrate: (a) Field emission scanning electron microscopy (FE-SEM) image of prepared Au nanoparticles; (b) FE-SEM image of prepared Au@Ag core-shell nanoparticles; (c) Low-magnification high-resolution transmission electron microscopy (HR-TEM) image of Au@Ag; (d) High-magnification HR-TEM images of Au@Ag; (e) Low-magnification FE-SEM image of glass nanofibrous paper; (f) High-magnification FE-SEM image of the glass nanofibrous paper substrate; (g) Low-magnification FE-SEM image of Au@Ag-pLL assembled on the glass nanofibrous paper substrate; (h) High-magnification FE-SEM image of Au@Ag-pLL assembled on the glass nanofibrous paper substrate.

water at pH 2.0. The sample was then loaded onto the cartridge at a flow rate of 2–3 mL/min. After drying under vacuum, the sample was sequentially eluted off the cartridge with 4 mL of MeOH and 4 mL of 5% NH_3 in MeOH. The eluate was evaporated to dryness under a gentle nitrogen stream and re-constituted in 200 μL of AcN/water (5/95, v/v). A further cleaning step was performed using a 0.22 μm centrifugal filter (VWR International, PA, USA) before LC-MS analysis.

Theoretical calculation simulations: Density functional theory (DFT) calculations were used to confirm vibrational band assignments for methamphetamine ($C_{10}H_{15}N$). All the quantum chemical calculations were performed using DFT with the BP86 functional and 6–311G(d) basis set employing the Gaussian 09 and GaussView 3.09 program package (Kohn et al., 1996; P. Hohenberg, 1964). The calculations were performed without any symmetry restrictions.

3. Results and discussion

3.1. Novel substrate for SERS sensors

Au@Ag core-shell nanoparticles were synthesized to combine the strong SERS effect of Ag with the well-known stability of Au (Li et al., 2017). It has also been proposed that plasmonic Au@Ag core-shell nanomaterials have a better SERS effect than single-component Au or Ag due to their resonant behaviour (Li et al., 2017). The synthesized Au@Ag was characterized by ultraviolet-visible (UV–vis) spectrometry (Figure S1), as well as field emission scanning electron microscopy (FE-SEM) and high-resolution transmission electron microscopy (HR-TEM) (Fig. 2). Figure S1 shows the UV–vis spectra of AuNPs and Au@Ag. Compared with the absorption peak of AuNPs, the peak of the Au@Ag solution was blue-shifted. As shown in Fig. 2b and c, the average diameter of Au@Ag was approximately 40 nm, exhibiting a uniform size. We also obtained a more detailed Au@Ag particle size distribution image through HR-TEM (see Figure S2), which demonstrated that the majority of the diameter sizes of Au@Ag ranged from 37 to 43 nm (16/21).

The GNFP (8 mm × 8 mm) provided an enhanced surface area, leading to improvements in both sensitivity and dynamic range (as a function of the increased number of noble metal core-shell nanoparticles that could be modified on its surface). The surface topography of the GNFP was determined by FE-SEM (Fig. 2e and f), showing that a highly porous three-dimensional matrix was formed. When compared to two-dimensional planar substrates (Li et al., 2017), nanofibrous paper substrates, with a hierarchical structure of nanoparticles adsorbed onto the fibril matrix, exhibited an increased surface area and enhanced the absorption capacity for easy access of analytes. By absorbing the Au@Ag-pLL solution, the SERS GNFP could be easily fabricated (see Scheme 1).

Here, we used pLL to attach Au@Ag to the paper matrix by exploiting its positively charged amine functional groups and its low Raman scattering cross-section. pLL was readily absorbed onto the paper at room temperature without any other treatment, providing an excellent mediator for the physisorption and ionic stabilization of the negatively charged Au@Ag on the glassy paper in a single step.

According to a previous report (Fang et al., 2015), the assembly times of glass in pLL and nanoparticle solutions were optimized at 10 min and 30 h, respectively. Using characterization of low-magnification (Fig. 2g) and high-magnification (Fig. 2h) FE-SEM images, the experimental results show that the Au@Ag core-shell nanoparticles have been effectively loaded on GNFP with pLL. To investigate the reproducibility of the SERS platform, 8 different SERS substrates were used to measure 100 nM CV standards. Fig. 3a shows that the 8 different spectra were consistent, with a strong peak at 1620 cm^{-1}, showing a relative standard deviation (RSD) of ~5%.

Given that an ideal sensor substrate should be stable for long-term storage, we compared the SERS signals from a freshly prepared Au@Ag assembled on the GNFP substrate with the same substrate following storage under atmospheric conditions for one or two months. As shown in Fig. 3, 2 μL of 100 nM CV was analysed on the freshly prepared Au@Ag-pLL-GNFP SERS substrate (No. 3) and from a substrate prepared one month (No. 2) and two months (No. 1) earlier. Raman spectra were obtained using a portable Raman spectroscopy system (i-Raman portable Raman spectrometer, B&W Tek, USA) using a high quantum efficiency charge-coupled device (CCD) array detector. A 785 nm laser was used for excitation. The collection parameters of each SERS spectrum included an exposure time of 5000 ms and integrating 3 times over each spec-

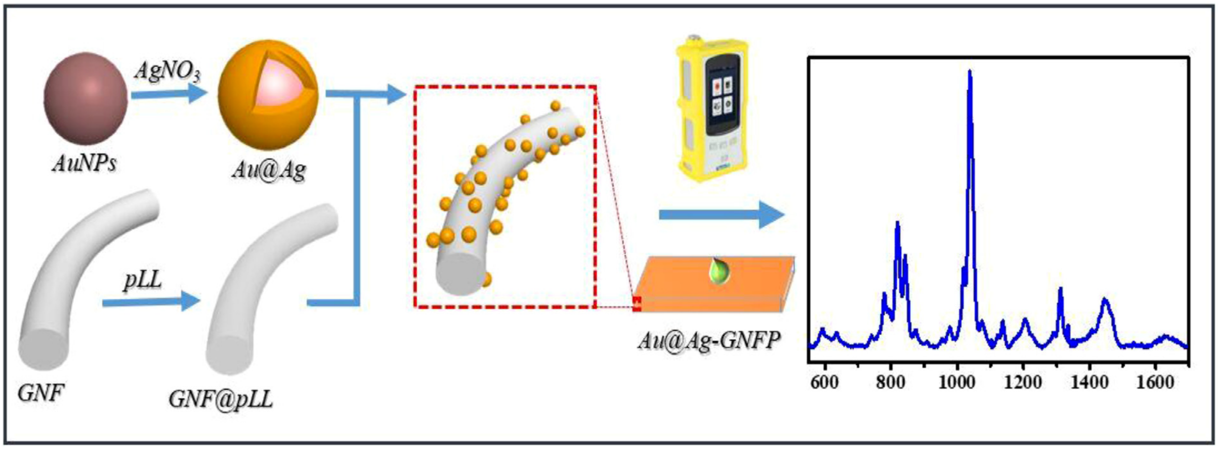

Scheme 1. Schematic illustration of the self-assembly of Au@Ag on a glass nanofibrous paper (GNFP) SERS substrate.

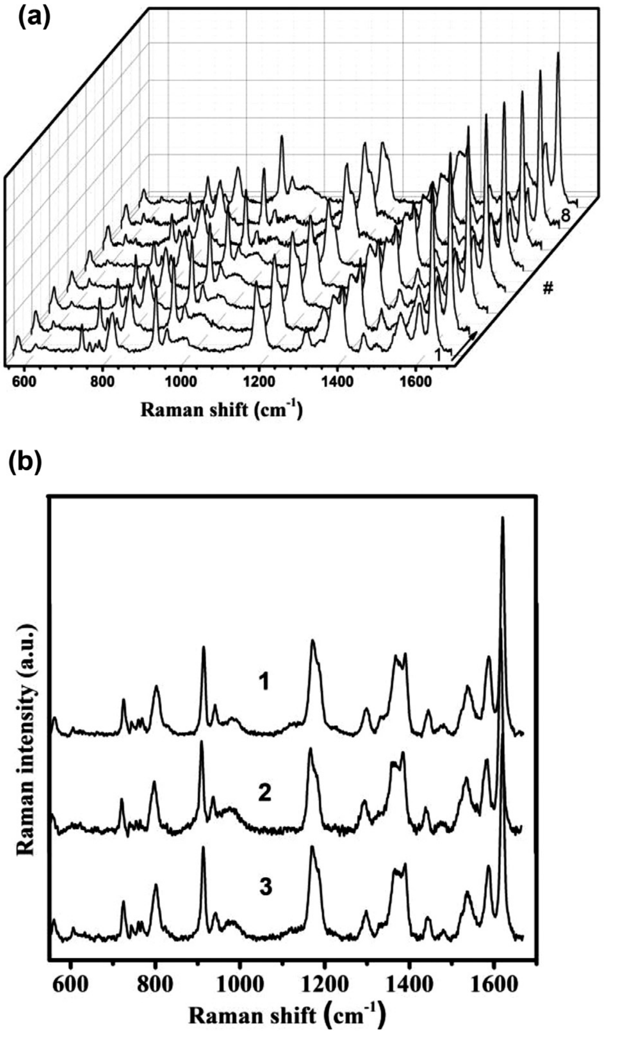

Fig. 3. (a) SERS spectra of CV (100 nM) acquired from 8 different SERS substrates within a SERS array, showing a high degree of reproducibility; (b) SERS spectra (λex = 785 nm) of CV (100 nM) acquired from a freshly prepared Au@Ag-pLL-GNFP SERS substrate (No. 3) and from a substrate prepared one month (No. 2) and two months (No. 1) earlier, showing good long-term stability of the nanofibrous paper-Au@Ag assembly.

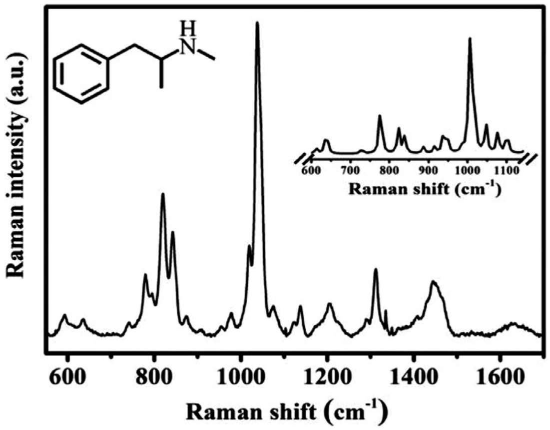

Fig. 4. SERS spectra of methamphetamine measured on Au@Ag-modified glass nanofibrous paper substrate. The inset shows the SERS spectra from DFT simulations. The powder spectra are provided in Fig. S3.

trum. The results demonstrated no significant decrease in the signal intensity, with a Raman peak at 1620 cm^{-1}, showing an RSD of ~5.9%.

3.2. Detection of illicit drugs in solutions

We used Au@Ag-pLL assembled on glass nanoporous paper substrates for SERS detection of methamphetamine, as shown in Fig. 4. Compared with the theoretical Raman spectra (Fig. 4 inset) and the powder spectra (Figure S3), the SERS spectra of methamphetamine show a close correspondence. The SERS bands were also compared with the theoretical predictions and vibrations as shown in Table S1, which were consistent with assignments made in previous investigations (Kline et al., 2016). The molecular structures of the analytes are presented in Fig. 4 as an aid for visualizing the vibrational mode assignments. As shown in the Raman spectra in Table S1, methamphetamine can be differentiated using five bands at 619 cm^{-1}, 835 cm^{-1}, 1001 cm^{-1}, 1016 cm^{-1} and 1602 cm^{-1}, although in our work, we found the strongest signal band at 1016 cm^{-1} to be analytically most useful.

To illustrate the analytical capability of the SERS-active substrate for illicit drug detection, we carried out the detection of methamphetamine in a combined qualitative and quantitative way.

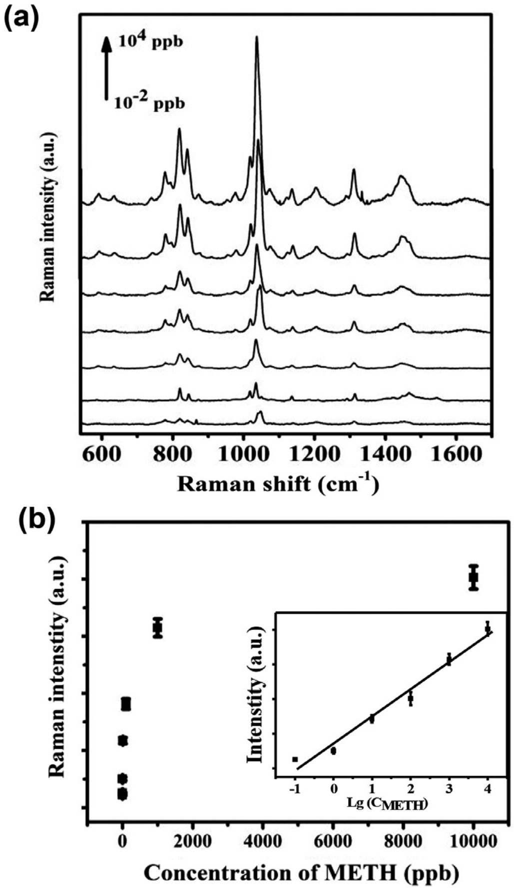

Fig. 5. SERS assay performance of different concentrations of (a) methamphetamine (0.01 to 10,000 ppb) on Au@Ag-pLL assembled on the glass nanofibrous paper substrate. (b) Standard curve of the corresponding peak intensities at 1016 cm^{-1} and ΔI_{1016} as a function of drug concentration.

First, 2 µL of the methamphetamine solution at a series of standard concentrations (0.01, 0.1, 1.0, 10.0, 100.0, 1000.0, and 10,000.0 ppb) in anhydrous ethanol were analysed on the SERS-enabled paper substrate. As the solvent evaporated, the analytes were spread evenly on the SERS-active layer on the sensor (Scheme 1). Raman spectra were obtained using a portable Raman spectroscopy system (i-Raman portable Raman spectrometer, B&W Tek, USA) using a high quantum efficiency CCD array detector. A 785 nm laser was used for excitation. The collection parameters of each SERS spectrum included an exposure time of 5000 ms and integrating 3 times over each spectrum.

Raman spectra of different concentrations of methamphetamine were obtained using the characteristic band at 1016 cm^{-1}. Fig. 5a indicates that the intensity of this signal increased for methamphetamine concentrations between 0.01 and 10,000.0 ppb (with the baseline subtracted from all the Raman spectra).

Fig. 5b shows the relationship between changes in the Raman intensity of methamphetamine with increasing methamphetamine concentrations, giving an excellent linear correlation (r^2=0.99) with the logarithmic concentration of methamphetamine ranging from 10^{-1} ppb to 10^4 ppb, as presented in the inset of Fig. 5b. The limit of detection was estimated to be 7.2 ppt (3 standard deviations above the mean of the baseline).

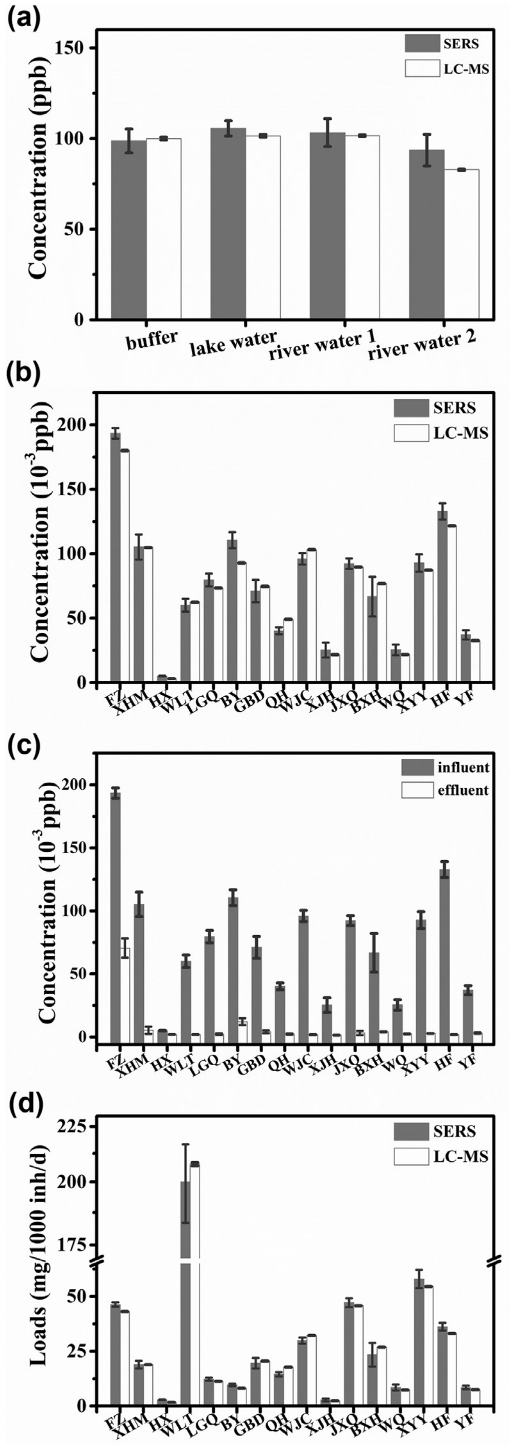

Fig. 6. (a) Detection of 100 ppb methamphetamine in different matrices (buffer, lake and river water) using the SERS sensors (black) and LC-MS (white) as the gold-standard reference method; (b) normalized methamphetamine concentrations in wastewater treatment plants measured using the SERS sensor (white) and HPLC-MS/MS; (black), as reference (see also Table S3); (c) normalized concentrations of methamphetamine determined by the SERS sensor in influent (black) and effluent (white) from wastewater treatment plants in Beijing, demonstrating the effectiveness of the wastewater treatment process (see Table S3); (d) estimated average loads of methamphetamine where wastewater samples were collected (see Table S4). (Notes: FZ, Fangzhuang; XHM, Xiaohongmen; HX, Hexi; WLT, Wulituo; LGQ, Lugouqiao; BY, Beiyuan; GBD, Gaobeidian; QH, Qinghe; WJC, Wujiacun; XJH, Xioajiahe; JXQ, Jiuxianqiao; BXH, Beixiaohe; WQ, Wenquan; XYY, Xiaoyueyuan; HF, Huaifang; YF, Yongfeng).

3.3. Evaluation of the drug concentration with SERS sensors by analysis of surface water

In order to investigate the efficacy of the sensor for the detection of real samples, we present preliminarily results that verified the feasibility of analysing surface water, including lake water and river water samples. The surface water samples were first filtered with 0.22 µm membrane filters. Then, 100 ppb methamphetamine was spiked into the different types of aqueous samples including buffer, lake sample and river samples, as shown in Fig. 6a (using LC-MS measurements as our gold-standard reference technique). The results from the buffer sample corresponded well with the measured concentrations in the lake and river samples, including the Pearl River and Wanquan River, as shown in Table S2.

3.4. Evaluation of community drug consumption with SERS sensors at wastewater treatment plants

We also analysed methamphetamine concentrations in the wastewater collected from 16 influent and effluent pipes in wastewater treatment plants in Beijing, again normalized by the daily flow rate of sewage at each plant. Fig. 6b Fig. 6b and Fig. 6d demonstrated the concentrations of methamphetamine in sewage in Beijing, and estimated average loads of methamphetamine, where wastewater samples were collected from influent (detailed data in the Tables S3 and S4). As shown in Table S3, methamphetamine was present in all of the influents, with concentrations ranging from 3.10 ppt to 180.0 ppt. The high concentration level of methamphetamine in influents suggests a wide use of methamphetamine in Beijing. Table S3 shows that higher methamphetamine daily drug loadings per daily flow rate are present at the five sites (Xiaohongmen, Gaobeidian Qinghe, Jiuxianqiao, and Huaifang) that are located in more central districts of Beijing, as shown in Fig. 1, closest to the business and entertainment centres with the highest population densities. Wenquan and Yongfeng are the farthest from the centre of the city and showed the lowest daily drug load of methamphetamine in our sampling periods. The drug load was also low at Xiaojiahe and Hexi, which, although not far from the urban centre, receive sewage from the suburbs.

Finally, we also found that the removal efficiencies of methamphetamine were efficient in the wastewater treatment plants by comparing the influent with effluent samples, as shown in Fig. 6b and Table S3, again using data that were normalized by the flow rate. As shown in Fig. 6c, the removal efficiencies for methamphetamine were typically $>$ 89% (with the exception of the Fangzhuang (63.5%) and Hexi (60.3%) plants). Similarly, high methamphetamine removal efficiencies have been observed in the literature elsewhere (Loganathan et al., 2009; Postigo et al., 2010).

4. Conclusion

In summary, we present the development of methods for the fabrication of SERS substrates comprising glass nanoporous paper synthesized by electrospinning, functionalized with Au@Ag core-shell nanoparticles. The substrates serve as simple SERS sensors with negligible background interference, providing high sensitivity, good reproducibility and excellent stability. The sensors were used for the detection of methamphetamine in water treatment plants in Beijing district, and the results were in close agreement with those obtained by a gold-standard mass spectrometry method as a reference. This application of SERS sensors demonstrates an innovative technology for the evaluation of community-wide methamphetamine consumption. The results also showed the effective removal of the drug, measured as the difference between influx and efflux, at the sampled wastewater treatment plants. The SERS sensors provided a clear demonstration of a new WBE tool that could have generic application to a range of public health issues, including those for the rapid monitoring of community drug use, local environmental pollution and markers for infectious diseases. In addition, chiral sensors should be further explored in the future with the increasing attention on chiral compounds analysis in wastewater.

Declaration of Competing Interest

The authors declare no competing financial interest.

Acknowledgement

The authors acknowledge support from a UK NERC Fellowship (NE/R013349/2), Royal Academy of Engineering Frontier Follow-up grant (FF\1920\1\36) on paper sensors, and the National Science Foundation of China (NSFC) (no. 41371442 and 41401566). K.M. is greatful for a scholarship supported by Graduate School of Peking University (no. 20180211). JC also acknowledges GCRF and EPSRC funding on paper-based sensors through EPSRC EP/R01437X/1. Data underlying this paper can be accessed at http://doi.org/10.17862/cranfield.rd.13173251. Data underlying this paerp.

Supplementary materials

Supplementary material associated with this article can be found, in the online version, at doi:10.1016/j.watres.2020.116559.

References

Abbas, A., Brimer, A., Slocik, J.M., Tian, L., Naik, R.R., Singamaneni, S., 2013. Multifunctional analytical platform on a paper strip: separation, preconcentration, and subattomolar detection. Anal. Chem. 85 (8), 3977–3983.

Ahmed, A., Gordon, R., 2012. Single molecule directivity enhanced raman scattering using nanoantennas. Nano Lett. 12 (5), 2625–2630.

Bell, S.E., Sirimuthu, N.M., 2008. Quantitative surface-enhanced Raman spectroscopy. Chem. Soc. Rev. 37 (5), 1012–1024.

Brown, R.J.C., Milton, M.J.T., 2008. Nanostructures and nanostructured substrates for surface—enhanced Raman scattering (SERS). J. Raman Spectrosc. 39 (10), 1313–1326.

Castiglioni, S., Bijlsma, L., Covaci, A., Emke, E., Hernández, F., Reid, M., Ort, C., Thomas, K.V., van Nuijs, A.L.N., De, V.P., 2013. Evaluation of uncertainties associated with the determination of community drug use through the measurement of sewage drug biomarkers. Environ. Sci. Technol. 47 (3), 1452–1460.

Castiglioni, S., Borsotti, A., Senta, I., Zuccato, E., 2015. Wastewater analysis to monitor spatial and temporal patterns of use of two synthetic recreational drugs, ketamine and mephedrone, in Italy. Environ. Sci. Technol. 49 (9), 5563–5570.

Castrignanò, E., Yang, Z., Bade, R., Baz-Lomba, J.A., Castiglioni, S., Causanilles, A., Covaci, A., Gracia-Lor, E., Hernandez, F., Kinyua, J., McCall, A.-K., van Nuijs, A.L.N., Ort, C., Plósz, B.G., Ramin, P., Rousis, N.I., Ryu, Y., Thomas, K.V., de Voogt, P., Zuccato, E., Kasprzyk-Hordern, B., 2018. Enantiomeric profiling of chiral illicit drugs in a pan-European study. Water Res. 130, 151–160.

Chen, C.E., Zhang, H., Ying, G.G., Jones, K.C., 2013. Evidence and recommendations to support the use of a novel passive water sampler to quantify antibiotics in wastewaters. Environ. Sci. Technol. 47 (23), 13587–13593.

Cheng, C., Yan, B., Wong, S.M., Li, X., Zhou, W., Yu, T., Shen, Z., Yu, H., Fan, H.J., 2010. Fabrication and SERS performance of silver-nanoparticle-decorated Si/ZnO nanotrees in ordered arrays. ACS Appl. Mater. Interfaces 2 (7), 1824–1828.

Cheng, M.L., Tsai, B.C., Yang, J., 2011. Silver nanoparticle-treated filter paper as a highly sensitive surface-enhanced Raman scattering (SERS) substrate for detection of tyrosine in aqueous solution. Anal. Chim. Acta 708 (1–2), 89–96.

Cyranoski, D., 2018. Chinese cities scan sewers for signs of illegal drug use. Nature 559 (7714), 310–311.

Du, P., Li, K., Li, J., Xu, Z., Fu, X., Yang, J., Zhang, H., Li, X., 2015. Methamphetamine and ketamine use in major Chinese cities, a nationwide reconnaissance through sewage-based epidemiology. Water Res. 84, 76–84.

Du, P., Thai, P.K., Bai, Y., Zhou, Z., Xu, Z., Zhang, X., Wang, J., Zhang, C., Hao, F., Li, X., 2019. Monitoring consumption of methadone and heroin in major Chinese cities by wastewater-based epidemiology. Drug Alcohol 205, 107532.

Du, P., Zhou, Z., Bai, Y., Xu, Z., Gao, T., Fu, X., Li, X., 2017. Estimating heroin abuse in major Chinese cities through wastewater-based epidemiology. Sci. Total Environ. 605, 158–165.

Fang, W., Zhang, X., Chen, Y., Wan, L., Huang, W., Shen, A., Hu, J., 2015. Portable SERS-enabled micropipettes for microarea sampling and reliably quantitative detection of surface organic residues. Anal. Chem. 87 (18), 9217–9224.

Harman, C., Reid, M., Thomas, K.V., 2011. In situ calibration of a passive sampling device for selected illicit drugs and their metabolites in wastewater, and subsequent year-long assessment of community drug usage. Environ. Sci. Technol. 45 (13), 5676–5682.

He, D., Hu, B., Yao, Q.F., Wang, K., Yu, S.H., 2009. Large-scale synthesis of flexible free-standing SERS substrates with high sensitivity: electrospun PVA nanofibers embedded with controlled alignment of silver nanoparticles. ACS Nano 3 (12), 3993–4002.

Huang, X.-.B., Wu, S.-.H., Hu, H.-.C., Sun, J.-.J., 2020. AuNanostar@4-MBA@Au core–shell nanostructure coupled with exonuclease III-assisted cycling amplification for ultrasensitive SERS detection of ochratoxin A. ACS Sens. 5 (8), 2636–2643.

Ji, W., Kitahama, Y., Xue, X., Zhao, B., Ozaki, Y., 2012. Generation of pronounced resonance profile of charge-transfer contributions to surface-enhanced Raman scattering. J. Phys. Chem. C 116 (3), 2515–2520.

Kline, N.D., Tripathi, A., Mirsafavi, R., Pardoe, I., Moskovits, M., Meinhart, C., Guicheteau, J.A., Christesen, S.D., Iii, A.W.F., 2016. Optimization of surface-enhanced Raman spectroscopy conditions for implementation into a microfluidic device for drug detection. Anal. Chem. 88 (21), 10513–10522.

Kneipp, J., Kneipp, H., Kneipp, K., 2008. SERS—a single-molecule and nanoscale tool for bioanalytics. Chem. Soc. Rev. 37 (5), 1052–1060.

Kohn, W., And, A.D.B., Parr, R.G., 1996. Density functional theory of electronic structure. J. Phys. Chem. 31 (31), 12974–12980.

Kudelski, A., 2005. Raman studies of rhodamine 6G and crystal violet sub-monolayers on electrochemically roughened silver substrates: do dye molecules adsorb preferentially on highly SERS-active sites? Chem. Phys. Lett. 414 (4), 271–275.

Lee, C.H., Hankus, M.E., Tian, L., Pellegrino, P.M., Singamaneni, S., 2011. Highly sensitive surface enhanced Raman scattering substrates based on filter paper loaded with plasmonic nanostructures. Anal. Chem. 83 (23), 8953–8958.

Lee, C.H., Tian, L., Singamaneni, S., 2010. Paper-based SERS swab for rapid trace detection on real-world surfaces. ACS Appl. Mater. Interfaces 2 (12), 3429–3435.

Lee, J.-.C., Kim, W., Choi, S., 2017. Fabrication of a SERS-encoded microfluidic paper-based analytical chip for the point-of-assay of wastewater. Int. J. Precis. Eng. Manuf.-Green Technol. 4 (2), 221–226.

Li, J.F., Zhang, Y.J., Ding, S.Y., Panneerselvam, R., Tian, Z.Q., 2017. Core-shell nanoparticle-enhanced Raman spectroscopy. Chem. Rev. 117 (7), 5002–5069.

Lin, J., Shang, Y., Li, X., Yu, J., Wang, X., Guo, L., 2016. Ultrasensitive SERS detection by defect engineering on single Cu_2O superstructure particle. Adv. Mater. 29 (5) UNSP 1604797.

Loganathan, B., Phillips, M., Mowery, H., Jones-Lepp, T.L., 2009. Contamination profiles and mass loadings of macrolide antibiotics and illicit drugs from a small urban wastewater treatment plant. Chemosphere 75 (1), 70–77.

Mao, K., Ma, J., Li, X., Yang, Z., 2019. Rapid duplexed detection of illicit drugs in wastewater using gold nanoparticle conjugated aptamer sensors. Sci. Total Environ. 688, 771–779.

Mao, K., Min, X., Zhang, H., Zhang, K., Cao, H., Guo, Y., Yang, Z., 2020. Paper-based microfluidics for rapid diagnostics and drug delivery. J. Control. Release 322, 187–199.

Markosian, C., Mirzoyan, N., 2019. Wastewater-based epidemiology as a novel assessment approach for population-level metal exposure. Sci. Total Environ. 689, 1125–1132.

Martinez, A.W., Phillips, S.T., Carrilho, E., Iii, S.W.T., Sindi, H., Whitesides, G.M., 2008. Simple telemedicine for developing regions: camera phones and paper-based microfluidic devices for real-time, off-site diagnosis. Anal. Chem. 80 (10), 3699–3707.

Martinez, A.W., Phillips, S.T., Whitesides, G.M., Carrilho, E., 2010. Diagnostics for the developing world: microfluidic paper-based analytical devices. Anal. Chem. 82 (1), 3–10.

Meng, Y., Lai, Y., Jiang, X., Zhao, Q., Zhan, J., 2013. Silver nanoparticles decorated filter paper via self-sacrificing reduction for membrane extraction surface-enhanced Raman spectroscopy detection. Analyst 138 (7), 2090–2095.

Niaz, K., Pietchman, T., Davis, P., Carpentier, C., Raithelhuber, M., 2017. World Drug Report 2017.

Hohenberg, P., Kohn, W., 1964. The inhomogeneous electron gas. Phys. Rev. 136 (B), 864–871.

Peccia, J., Zulli, A., Brackney, D.E., Grubaugh, N.D., Kaplan, E.H., Casanovas-Massana, A., Ko, A.I., Malik, A.A., Wang, D., Wang, M., Warren, J.L., Weinberger, D.M., Arnold, W., Omer, S.B., 2020. Measurement of SARS-CoV-2 RNA in wastewater tracks community infection dynamics. Nat. Biotechnol. 38 (10), 1164.

Polavarapu, L., Liz-Marzán, L.M., 2013. Towards low-cost flexible substrates for nanoplasmonic sensing. Phys. Chem. Chem. Phys. 15 (15), 5288–5300.

Polavarapu, L., Porta, A.L., Novikov, S.M., Coronado-Puchau, M., Liz-Marzán, L.M., 2014. Pen-on-paper approach toward the design of universal surface enhanced raman scattering substrates. Small 10 (15), 3065–3071.

Postigo, C., López de Alda, M.J., Barceló, D., 2010. Drugs of abuse and their metabolites in the Ebro river basin: occurrence in sewage and surface water, sewage treatment plants removal efficiency, and collective drug usage estimation. Environ. Int. 36 (1), 75–84.

Reid, M.J., Bazlomba, J.A., Ryu, Y., Thomas, K.V., 2014. Using biomarkers in wastewater to monitor community drug use: a conceptual approach for dealing with new psychoactive substances. Sci. Total Environ. 487 (14), 651–658.

Reilly, T.H., Corbman, J.D., Rowlen, K.L., 2007. Vapor deposition method for sensitivity studies on engineered surface-enhanced Raman scattering-active substrates. Anal. Chem. 79 (13), 5078–5081.

Ren, W., Fang, Y., Wang, E., 2011. A Binary Functional substrate for enrichment and ultrasensitive SERS spectroscopic detection of folic acid using graphene oxide/Ag nanoparticle hybrids. ACS Nano 5 (8), 6425–6433.

Rousis, N.I., Gracia-Lor, E., Zuccato, E., Bade, R., Baz-Lomba, J.A., Castrignanò, E., Causanilles, A., Covaci, A., de Voogt, P., Hernàndez, F., Kasprzyk-Hordern, B., Kinyua, J., McCall, A.-.K., Plósz, B.G., Ramin, P., Ryu, Y., Thomas, K.V., van Nuijs, A., Yang, Z., Castiglioni, S., 2017. Wastewater-based epidemiology to assess pan-European pesticide exposure. Water Res. 121, 270–279.

Shen, A., Chen, L., Xie, W., Hu, J., Zeng, A., Richards, R., Hu, J., 2010. Triplex Au-Ag-C core-shell nanoparticles as a novel Raman label. Adv. Funct. Mater. 20 (6), 969–975.

Sims, N., Kasprzyk-Hordern, B., 2020. Future perspectives of wastewater-based epidemiology: monitoring infectious disease spread and resistance to the community level. Environ. Int. 139, 105689.

Su, J., Wang, D., Nörbel, L., Shen, J., Zhao, Z., Dou, Y., Peng, T., Shi, J., Mathur, S., Fan, C., 2017. Multicolor gold-silver nano-mushrooms as ready-to-use SERS probes for ultrasensitive and multiplex DNA/miRNA detection. Anal. Chem. 89 (4), 2531–2538.

Wang, H., And, C.S.L., Halas, N.J., 2005. Nanosphere arrays with controlled sub-10-nm gaps as surface-enhanced Raman spectroscopy substrates. J. Am. Chem. Soc. 127 (43), 14992–14993.

Xie, W., Herrmann, C., Kömpe, K., Haase, M., Schlücker, S., 2011. Synthesis of bifunctional Au/Pt/Au Core/shell nanoraspberries for in situ SERS monitoring of platinum-catalyzed reactions. J. Am. Chem. Soc. 133 (48), 19302–19305.

Xu, L., Zhang, H., Tian, Y., Jiao, A., Chen, F., Chen, M., 2019. Photochemical synthesis of ZnO@Au nanorods as an advanced reusable SERS substrate for ultrasensitive detection of light-resistant organic pollutant in wastewater. Talanta 194, 680–688.

Yang, Z., Castrignanò, E., Estrela, P., Frost, C.G., Kasprzyk-Hordern, B., 2016. Community sewage sensors towards evaluation of drug use trends: detection of cocaine in wastewater with DNA-directed immobilization aptamer sensors. Sci. Rep. 6, 21024.

Yap, F.L., Thoniyot, P., Krishnan, S., Krishnamoorthy, S., 2012. Nanoparticle cluster arrays for high-performance SERS through directed self-assembly on flat substrates and on optical fibers. ACS Nano 6 (3), 2056–2070.

Yu, W.W., White, I.M., 2010. Inkjet printed surface enhanced Raman spectroscopy array on cellulose paper. Anal. Chem. 82 (23), 9626–9630.

Zhang, K., Ji, J., Fang, X., Yan, L., Liu, B., 2015. Carbon nanotube/gold nanoparticle composite-coated membrane as a facile plasmon-enhanced interface for sensitive SERS sensing. Analyst 140 (1), 134–139.

Zuccato, E., Chiabrando, C., Castiglioni, S., Bagnati, R., Fanelli, R., 2008. Estimating community drug abuse by wastewater analysis. Environ. Health Perspect. 116 (8), 1027–1032.

Zuccato, E., Chiabrando, C., Castiglioni, S., Calamari, D., Bagnati, R., Schiarea, S., Fanelli, R., 2005. Cocaine in surface waters: a new evidence-based tool to monitor community drug abuse. Environ. Health-Glob. 4 (4), 14.